

# Effect of electron beam treatment on adhesion of Ta/polymeric low-k interface

Damayanti, M.; Prasad, K.; Chen, Zhe; Zhang, Sam; Jiang, Ning; Gan, Zhenghao; Chen, Zhong; Mhaisalkar, Subodh Gautam

2006

Gan, Z., Chen, Z., Mhaisalkar, S. G., Damayanti, M., Chen, Z., Prasad, K., et. al. (2006). Effect of electron beam treatment on adhesion of Ta/polymeric low-k interface. Applied physics letters, 88 (23).

<https://hdl.handle.net/10356/79990>

<https://doi.org/10.1063/1.2212533>

---

© 2006 American Institute of Physics. This paper was published in Applied Physics Letters and is made available as an electronic reprint (preprint) with permission of American Institute of Physics. The paper can be found at the following DOI:

<http://dx.doi.org/10.1063/1.2212533>. One print or electronic copy may be made for personal use only. Systematic or multiple reproduction, distribution to multiple locations via electronic or other means, duplication of any material in this paper for a fee or for commercial purposes, or modification of the content of the paper is prohibited and is subject to penalties under law.

*Downloaded on 15 Aug 2024 00:27:09 SGT*

## Effect of electron beam treatment on adhesion of Ta/polymeric low-*k* interface

Zhenghao Gan,<sup>a)</sup> Zhong Chen, S. G. Mhaisalkar, and M. Damayanti  
*School of Materials Science and Engineering, Nanyang Technological University, Singapore 639798, Singapore*

Zhe Chen and K. Prasad  
*School of Electrical and Electronic Engineering, Nanyang Technological University, Singapore 639798, Singapore*

Sam Zhang  
*School of Mechanical and Aerospace Engineering, Nanyang Technological University, Singapore 639798, Singapore*

Jiang Ning  
*Institute of Microelectronics, 11 Science Park Road, Singapore 117685, Singapore*

(Received 22 August 2005; accepted 18 May 2006; published online 8 June 2006)

Reliability of the Cu/low-*k* structure is a serious concern since the metal/dielectric interface is generally weak. The adhesion of the Ta/polyarylene ether interfaces with and without electron beam (EB) treatment was investigated by four-point bending test, x-ray photoelectron spectroscopy, and density functional theory. Higher adhesion energy ( $G_c$ ) was achieved with low-dose EB treatment, attributed to the strong Ta-arene interaction. However, high-dose EB breaks the aromatic rings partially, resulting in fewer available sites for Ta-arene bonding, leading to lower adhesion. It is suggested that the amount of carbon atoms involved in bonding with the metal is the key to improve the Ta/polymer adhesion. © 2006 American Institute of Physics. [DOI: 10.1063/1.2212533]

Polymeric low-*k* dielectrics have been introduced in the Cu damascene structures as a result of increasing demand on integrated circuit (IC) device density and performance.<sup>1,2</sup> Porous polyarylene ether (PAE) has been proposed as one of the candidates because of its low dielectric constant (2.65–3.0) and high thermal stability (>425 °C).<sup>2,3</sup> A metallic barrier layer such as Ta is always employed to block Cu diffusion into the dielectrics.<sup>4</sup> Reliability of the Cu/low-*k* structure is a serious concern since the metal/dielectric interface is generally weak. Electron beam (EB) curing can effectively make the cage-like bonds of porous organosilicate glass (OSG) transfer to network bonds, thus improving adhesion property.<sup>5</sup> However, other work found that EB treatments on OSG did not improve interfacial adhesion significantly (<10%).<sup>6</sup> Previous study showed that EB treatment could reduce line-to-line leakage current in Cu/Ta/PAE interconnect comb structures, attributed to the reduced oxygen content at the Ta/PAE interface.<sup>7</sup> In this letter, we demonstrate that EB treatment with controlled dose could improve adhesion of the Ta/PAE interface. The underlying mechanism is revealed by x-ray photoelectron spectroscopy (XPS) analysis and density-functional theory (DFT) calculation.

The chemical structure of PAE precursor is shown as the inset in Fig. 1.<sup>2</sup> A 300-nm-thick PAE film was deposited on an 8-in.-diameter *p*-type Si(100) wafer using spin-on technique. A 25-nm-thick Ta layer was then deposited immediately by physical vapor deposition. The film thickness was confirmed by transmission electron microscopy (TEM) examination. Two other wafers with PAE film were exposed under EB in a vacuum chamber by employing an EB scan

system prior to Ta deposition. The doses for the EB exposure were 20  $\mu\text{C}/\text{cm}^2$  (low dose) and 40  $\mu\text{C}/\text{cm}^2$  (high dose), respectively, with the same energy (50 keV). XPS measurements were carried out to investigate interface chemistry and depth profile in a Kratos AXIS spectrometer<sup>8</sup> (UK) with the monochromatic Al  $K\alpha$  x-ray radiation at 1486.71 eV and base vacuum of  $\sim 10^{-9}$  Torr. The adhesion strength, in terms of critical energy release rate ( $G_c$ ) of the Ta/PAE interface, was quantified by four-point bending (4PB) technique.<sup>9</sup> For each case, ten samples were tested.

Figure 1 compares the XPS depth profile of Ta/PAE low-*k* interfaces. Small amount of Ta atoms may diffuse into the PAE film, mainly attributed to the porous characteristic of

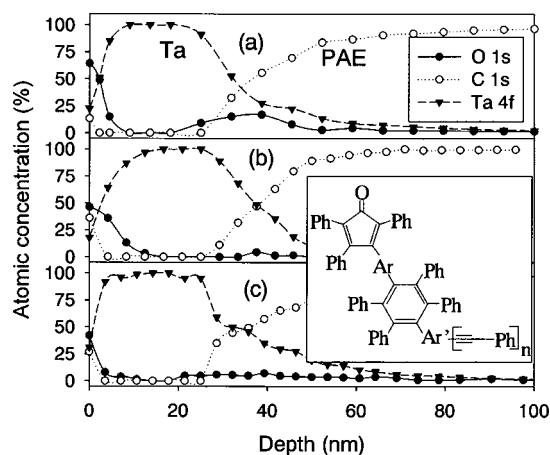

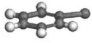


FIG. 1. XPS depth profile of Ta/PAE low-*k* interface: (a) without, (b) with EB treatment (20  $\mu\text{C}/\text{cm}^2$ ), and (c) with EB treatment (40  $\mu\text{C}/\text{cm}^2$ ). The inset shows the chemical structure of PAE precursor, where Ar and Ph are short for aryl and phenyl, respectively.

<sup>a)</sup> Author to whom correspondence should be addressed; FAX: +65-67909081; electronic mail: ezhgan@ntu.edu.sg

TABLE I. Comparison between experiments and DFT simulation.

	Experiments		DFT simulation		
	x (TaC <sub>x</sub> at interface)	G <sub>c</sub> (J/m <sup>2</sup> )		Binding energy	Estimated G <sub>c</sub> (J/m <sup>2</sup> )
without EB	~1.8	5.9±1.1	—	—	—
Low-dose EB	~2.3	8.1±0.5		-3.8 eV	9.4
High-dose EB	~0.2	4.0±0.6		-2.6 eV	6.4

PAE. Similar Ta diffusion was observed at the Ta/porous *a*-SiC:H interface.<sup>10</sup> It is clear that no inherent oxygen was detected in the bulk of the PAE film, mainly due to its low content less than the sensitivity of the XPS equipment. For the case without EB treatment [Fig. 1(a)], about 20% of the atoms located in the Ta/PAE interface are oxygen. This interfacial oxygen may be a result of oxygen/moisture absorption during process transfer from PAE deposition to physical vapor deposition (PVD) barrier deposition. Similar XPS spectra of PAE and the incorporation of oxygen were reported earlier.<sup>11</sup> Preliminary results showed that oxygen/moisture uptake would weaken the electrical characteristics in terms of leakage current and breakdown strength.<sup>7</sup> On the other hand, the O species were hardly detected at the Ta/PAE interface with EB treatments [Figs. 1(b) and 1(c)]. It is conceivable that high energy electrons would break the weakly bonded oxygen.

The  $G_c$  values of Ta/PAE interfaces obtained by 4PB in the current study were  $5.9 \pm 1.1$ ,  $8.1 \pm 0.5$ , and  $4.0 \pm 0.6$  J/m<sup>2</sup> with EB doses of 0, 20, and 40  $\mu\text{C}/\text{cm}^2$ , respectively (Table I). The error of the  $G_c$  value is caused by the variation in the critical flaw among test specimens due to the porous nature of the Ta/PAE interface. It is noted that the Ta layer was thin (25 nm); therefore, the plastic deformation effect should be negligible during the 4PB measurement.<sup>12</sup> The measured  $G_c$  values were also comparable to those of other Ta/low- $k$  interfaces.<sup>13</sup> It is interesting that the adhesion energy increased about 37% when EB dose was 20  $\mu\text{C}/\text{cm}^2$ , which could be attributed to the active PAE surface induced by the EB, thus improving the Ta-PAE bonding. However, with the higher-dose EB treatment,  $G_c$  value reduced by about one-third compared to the pristine case. One possible explanation may be the damage caused by the EB treatment. However, the higher EB dose of 40  $\mu\text{C}/\text{cm}^2$  in our study is much lower than that of immersing system in a conventional EB curing process ( $\sim 500$   $\mu\text{C}/\text{cm}^2$ ),<sup>14</sup> where no damage was observed under in-line field emission scanning electron microscopy.

Figure 2 gives the comparison of spectra deconvolution of C 1s for all cases at around 40 nm depth. For pristine interface [Fig. 2(a)], the spectrum could be deconvoluted into three components, corresponding to C–Ta (at 283.2 eV),<sup>4</sup> C–C (at 285 eV), and C–O bonds (at 287 eV), respectively. With EB treatments, either low dose [Fig. 2(b)] or high dose [Fig. 2(c)], the C–O bond is not detectable because the absorbed O species were removed by EB. In addition, the relative amount of C–Ta bonds increased with lower-dose EB treatment [Fig. 2(b)], whereas they decreased

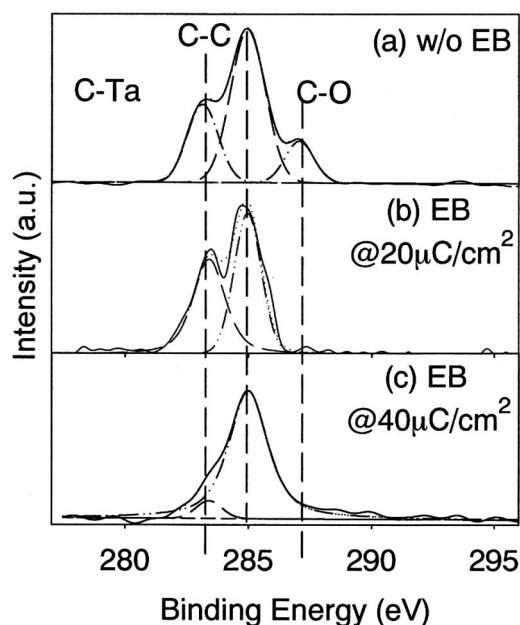


FIG. 2. Deconvolution of spectra: (a) C 1s without EB treatment, (b) C 1s with EB treatment (20  $\mu\text{C}/\text{cm}^2$ ), and (c) C 1s with EB treatment (40  $\mu\text{C}/\text{cm}^2$ ).

substantially with higher-dose EB treatment [Fig. 2(c)]. If we consider the TaC<sub>x</sub> compound formed at the interface, values of  $x$  are around 1.8, 2.3, and 0.2 for pristine, low-dose, and high-dose EB treatments, respectively (Table I). Several references have mentioned that the formation of C–Ta bonds at the interface can improve the adhesion.<sup>1,15</sup> Therefore fewer C–Ta bonds may be the main reason leading to the lower adhesion energy of the specimens with higher-dose EB treatment.

The Ta/PAE interfacial interaction involves the charge transfer complexes between the metal and the entire aromatic  $\pi$  system, previously proposed for Cr on pyromellitic dianhydride-oxydianiline (PMDA-ODA).<sup>16</sup> With the lower dose of EB treatment, the aromatic complexes at the PAE surface are more active and more Ta–C bonds will form, leading to a stronger interface. However, if a too high dosage is imposed, the C–C or C–H bonds may be partially broken, resulting in fewer available sites for Ta-arene bonding. Thus, with the higher-dose EB treatments, fewer carbon atoms will be bonded to Ta atoms as demonstrated by XPS (Fig. 2), leading to lower adhesion.

Here we present an energetic analysis from first principles calculation for the binding energy of a single Ta to a benzene complex [Fig. 3(c)] and that to a single C atom in the aromatic ring [Fig. 3(b)]. Following the method to calculate the cohesive energy,<sup>17</sup> the binding energy is derived by subtracting the energies of an isolated Ta atom and an isolated benzene molecule [Fig. 3(a)] from the total energy of the configuration shown in Fig. 3(b) and 3(c). The calculation using isolated benzene molecule and Ta(C<sub>6</sub>H<sub>6</sub>), in one way, is to save computational time but, in the other way, could get a preliminary insight on the Ta-arene interaction. Similar simplification was adopted by others to study the metal-arene compounds.<sup>18</sup> The calculations were performed using DFT-based CASTEP.<sup>19</sup> The exchange-correlation energy is described by GGA-PBE.<sup>20</sup> The Brillouin zone is sampled with a Monkhorst-Pack  $k$ -point grid.<sup>21</sup> The configurations

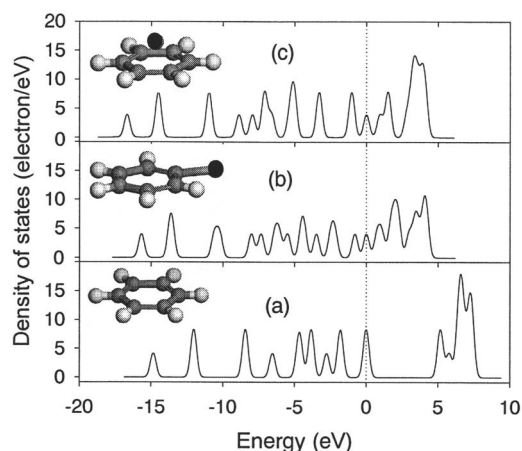


FIG. 3. DOS curves for (a) isolated benzene, (b) Ta side with benzene corresponding to high-dosage EB treatment, and (c) Ta on top of benzene corresponding to low-dosage EB treatment. The insets are the ball and stick models. Light: H atoms, grey: C atoms, and dark: Ta atoms. The positions of the Ta atoms relative to the aromatic ring have been optimized after geometrical relaxation.

shown in Fig. 3 are placed in a  $15 \times 15 \times 15 \text{ \AA}^3$  supercell. A  $[1 \times 1 \times 2]$   $k$ -point mesh was used with plane-wave cutoff at 260 eV. After relaxing the structure of Fig. 3(c), the Ta atom is exactly located above the center of the aromatic ring with Ta–C bond length of 2.16 Å, which agrees very well with the reported value of 2.205 Å in a TaC crystal.<sup>22</sup> The calculated binding energy for a single Ta-arene complex is  $-3.8 \text{ eV}$  [Fig. 3(c)], indicating that the system will be more stable after Ta binding to the benzene. It is interesting to estimate the macroscopic adhesion energy based on the calculated binding energy as follows. In Fig. 3(c), the C–C and C–H bond lengths are 1.39 and 1.09 Å, respectively. The area of a single arene is about  $6.44 \times 10^{-20} \text{ m}^2$ , giving an adhesion energy value of  $5.9 \times 10^{19} \text{ eV/m}^2$ , i.e.,  $9.4 \text{ J/m}^2$ . This value is  $\sim 16\%$  higher than the measured  $G_c$  of the low-dose EB treated Ta/PAE interface ( $8.1 \text{ J/m}^2$ ) and should be considered as an upper bound of  $G_c$  since the PAE is porous and its surface may not be fully covered by the arene repeating units. On the other hand, the calculated binding energy for Ta interacting with single C atom in the aromatic ring [Fig. 3(b)] is  $-2.6 \text{ eV}$  (Table I). The corresponding estimated  $G_c$  is  $6.4 \text{ J/m}^2$ , which is weaker than the Ta-arene interaction in Fig. 3(c).

Additional insight can be gleaned from the calculated density of states (DOS) of the different configurations (Fig. 3). The Fermi levels are set to 0 eV. It is seen that there is a band gap between 0 and 5 eV for the isolated benzene [Fig. 3(a)], which disappears after Ta atom is bonded to the benzene [Figs. 3(b) and 3(c)]. All the energy peaks in Ta-benzene curves [Figs. 3(b) and 3(c)] shift downwards in energy relative to the corresponding peak in the free benzene curve. However, the amount shifted is larger when the Ta

atom is on top of the arene [Fig. 3(c)], indicating that more C atoms are involved in bonding with the metal, corresponding to the lower-dose treated Ta/PAE interface. This is consistent with the larger  $x$  value of  $\text{TaC}_x$  compound by XPS, the higher microscopic binding energy by DFT calculation, and the higher macroscopic  $G_c$  by 4PB (Table I).

In summary, we demonstrated that different dosage of EB treatment could either improve or deteriorate adhesion of the Ta/PAE interface. The  $G_c$  values of Ta/PAE interfaces obtained by four-point bending are  $5.9 \pm 1.1$ ,  $8.1 \pm 0.5$ , and  $4.0 \pm 0.6 \text{ J/m}^2$  with EB doses of 0, 20, and  $40 \mu\text{C/cm}^2$ , respectively. Both DFT calculation and XPS analysis indicated that the amount of carbon atoms involved in bonding with the metal is the key to improve the Ta/polymer interfacial adhesion.

- <sup>1</sup>G. R. Yang, Y. P. Zhao, B. Wang, E. Barnat, J. McDonald, and T. M. Lu, *Appl. Phys. Lett.* **72**, 1846 (1998).
- <sup>2</sup>S. J. Martin, J. P. Godschalx, M. E. Mills, E. O. Shaffer, and P. H. Townsend, *Adv. Mater. (Weinheim, Ger.)* **12**, 1769 (2000).
- <sup>3</sup>J. C. Maisonobe, G. Passemard, C. Lacour, C. H. Lecornec, P. Motte, P. Noël, and J. Torres, *Microelectron. Eng.* **50**, 25 (2000).
- <sup>4</sup>C. J. Uchibori and T. Kimura, *J. Vac. Sci. Technol. B* **21**, 1513 (2003).
- <sup>5</sup>T. C. Chang, T. M. Tsai, P. T. Liu, C. W. Chen, and T. Y. Tseng, *Thin Solid Films* **469–470**, 383 (2004).
- <sup>6</sup>G. Kloster, T. Scherban, G. Xu, J. Blaine, B. Sun, and Y. Zhou, *Proceedings of the IEEE International Interconnect Technology Conference Burlingame, CA, 3–5 June 2002* (IEEE, New York, 2002), pp. 242–244.
- <sup>7</sup>Z. Chen, K. Prasad, Z. H. Gan, S. Y. Wu, S. S. Mehta, N. Jiang, S. G. Mhaisalkar, Rakesh Kumar, and C. Y. Li, *IEEE Electron Device Lett.* **26**, 448 (2005).
- <sup>8</sup>*AXIS Operating Manual* (Kratos, Manchester, UK, 2002), Chap. 9.
- <sup>9</sup>Z. H. Gan, S. G. Mhaisalkar, Z. Chen, S. Zhang, Z. Chen, and K. Prasad, *Surf. Coat. Technol.* **198**, 85 (2005).
- <sup>10</sup>F. Iacopi, Z. Tokei, Q. T. Le, D. Shamiryan, T. Conard, B. Brijs, U. Kreissig, M. Van Hove, and K. Maex, *J. Appl. Phys.* **92**, 1548 (2002).
- <sup>11</sup>A. Rajagopal, C. Gregoire, J. J. Lemaire, J. J. Pireaux, M. R. Baklanov, S. Vanhaelemeersch, K. Maex, and J. J. Waterloos, *J. Vac. Sci. Technol. B* **17**, 2336 (1999).
- <sup>12</sup>M. Lane, R. H. Dauskardt, A. Vainchtein, and H. Gao, *J. Mater. Res.* **15**, 2758 (2000).
- <sup>13</sup>R. Saxena, W. Cho, O. Rodriguez, W. N. Gill, J. L. Plawsky, T. Tsui, and S. Grunow, *Mater. Res. Soc. Symp. Proc.* **863**, B6.6 (2005).
- <sup>14</sup>M. Shimada, H. Miyajima, R. Nakata, M. Yamaguchi, J. Murase, and H. Hata, *IEEE International Semiconductor Manufacturing Symposium (ISSM), San Jose, CA, 8–10 October 2001* (IEEE, New York, 2001), pp. 325–328.
- <sup>15</sup>K. S. Kim, Y. C. Jang, H. J. Kim, Y. C. Quan, J. Choi, D. Jung, and N. E. Lee, *Thin Solid Films* **377–378**, 122 (2000).
- <sup>16</sup>R. Haight, R. C. White, B. D. Silverman, and P. S. Ho, *J. Vac. Sci. Technol. A* **6**, 2188 (1988).
- <sup>17</sup>M. Lazzari, A. Vittadini, and A. Selloni, *Phys. Rev. B* **63**, 155409 (2001).
- <sup>18</sup>R. Sahnoun and C. Mijoule, *J. Phys. Chem. A* **105**, 6176 (2001).
- <sup>19</sup>M. D. Segall, P. L. D. Lindan, M. J. Probert, C. J. Pickard, P. J. Hasnip, S. J. Clark, and M. C. Payne, *J. Phys.: Condens. Matter* **14**, 2717 (2002).
- <sup>20</sup>J. P. Perdew, K. Burke, and M. Ernzerhof, *Phys. Rev. Lett.* **77**, 3865 (1996).
- <sup>21</sup>H. J. Monkhorst and J. D. Pack, *Phys. Rev. B* **13**, 5188 (1976).
- <sup>22</sup>H. O. Pierson, *Handbook of Refractory Carbides and Nitrides: Properties, Characteristics, Processing and Applications* (Noyes, Park Ridge, NJ, 1996), p. 47.